Chinese Physics Letters

PAPER

Whispering Gallery Mode Lasing Performance's Evolution of Floating GaN Microdisks Varying with Their Thickness

To cite this article: Gangyi Zhu *et al* 2022 *Chinese Phys. Lett.* **39** 123401

Whispering Gallery Mode Lasing Performance's Evolution of Floating GaN Microdisks Varying with Their Thickness

Gangyi Zhu(朱刚毅)[1*], Mufei Tian(田沐霏)[1], M. Almokhtar[2], Feifei Qin(秦飞飞)[1], Binghui Li(李炳辉)[3], Mengyao Zhou(周梦谣)[1], Fei Gao(高菲)[1], Ying Yang(杨颖)[1], Xin Ji(纪鑫)[1], Siqing He(何丝情)[1], and Yongjin Wang(王永进)[1]

[1]*GaN Optoelectronic Integration International Cooperation Joint Laboratory of Jiangsu Province, College of Telecommunications and Information Engineering, Nanjing University of Posts and Telecommunications, Nanjing 210003, China*

[2]*Physics Department, Assiut University, Assiut 71516, Egypt*

[3]*State Key Laboratory of Luminescence and Applications, Changchun Institute of Optics Fine Mechanics and Physics, Chinese Academy of Sciences, Changchun 130033, China*

(Received 29 September 2022; accepted manuscript online 3 November 2022)

Optical gain and loss of microcavity greatly affect the quality of lasing, how to improve optical gain and decrease optical loss is of great significance for the preparation of laser. In this study, four types standard microdisks with different thicknesses of 2.2 µm, 1.9 µm, 1.7 µm, and 1.45 µm were fabricated by micromachining technology process to modulate optical gain and loss of microdisk lasing. The whispering gallery mode lasing in the ultraviolet range of GaN microdisk devices was investigated for these devices in order to clarify the effect of microdisk thickness on device characteristics. The quality factor Q and lasing mode number for different thicknesses are calculated from the stimulated spectra. The lifetimes of the exciton combination properties of the devices were observed using time-resolved PL spectroscopy. The lasing modes are modulated, and the lifetime decreases, while the Q factor of the devices first increases and then decreases with decreasing thickness. All these results are induced by optical gain and loss competition.

DOI: 10.1088/0256-307X/39/12/123401

GaN is attracting increasing attention because of its room-temperature wide direct band gap (up to 3.4 eV) and is a promising candidate for optoelectronic device applications,[1–3] especially for ultraviolet (UV) lasers. In recent years, optical microcavities have attracted much attention owing to their huge application potential and scientific significance and have been extensively researched. Various shapes of optical microcavities[4–6] have been investigated, including micro-ring cavities, microdisk cavities, microsphere cavities, and microcore ring cavities. These devices were form-dependent optical resonant cavities. Lasing devices are classified into random lasers,[7–11] Fabry–Pérot (FP) lasers[12–15] and whisper-gallery mode (WGM) lasers.[16–27] Among these devices, WGM lasing has the highest quality factor Q and a low lasing threshold because of the extremely weak optical loss resulting from total internal reflection at the boundary of the microcavity. WGM microcavities have been applied in nonlinear effects, ultra-low-threshold lasers, and high-sensitivity biochemical sensing.[28–30] Performance of WGM is directly controlled by the size of the cavity, the shape of boundary of the cavity, and the refractive index of the medium inside and outside the cavity. Therefore, studying the limitation effect of different cavity shapes, sizes, and refractive indices on lasing is of great significance for discussing and predicting cavity properties, as well as designing microcavities with specific properties. This study investigate the influence of microdisk thickness on its characteristics.

In this work, we fabricated a floating GaN microdisk with a diameter of 5 µm by inductively coupled plasma (ICP) etching and isotropic wet-etching silicon methods, and investigated WGM lasing in the ultraviolet range of a GaN microdisk. To clarify the effect of the microdisk thickness on the device characteristics, we used dry etching to further etch the devices for 30, 60, and 90 s. Thus, a cavity thickness-controlled device was fabricated. The optical performances of four devices with different thicknesses, including the quality factor Q, exciton combination lifetime, and lasing mode number, were studied.

Materials and Methods. A floating GaN microdisk was fabricated on a commercial GaN/Si substrate. The wafer consists of a 2.2 µm GaN layer and a 1600 µm silicon substrate. The fabrication process for the floating GaN microdisks is shown in Fig. 1. First, SiO_2 microspheres were spin-coated on the GaN layer (step a), and then the top surface of the wafer was etched down to the silicon layer by ICP etching (step b). The parameters of ICP etching were as follows: Chlorine flow rate is 40 sccm, boron trichloride flow rate is 4 sccm, power is 300 W, pressure is 4 mTorr, etching time is 8 min, etching rate of GaN is approximately 0.575 µm/min, and etching thickness of GaN is approximately 2.2 µm. After removing the SiO_2 micro-

*Corresponding authors. Email: zhugangyi@njupt.edu.cn

spheres (step c), HNF solution (HF:HNO_3 = 1:9) isotropic wet etching of silicon was used to undercut the GaN microdisk and generate an air gap under the GaN microdisk (step d). When silicon was etched, a suspended GaN microdisk was created. The relative refractive index of the floating GaN microdisks was significantly improved (2.6/1) compared with that of the non-suspended GaN microdisks (2.6/3.4). Light confinement was improved in the vertical direction of the manufactured floating GaN microdisk owing to the low light loss caused by the removal of the silicon substrate. After the fabrication of GaN cavity, further ICP etching was used to control the thickness of the cavity (step e). Thus, four standard devices with different thicknesses of 2.2 µm, 1.9 µm, 1.7 µm, and 1.45 µm were fabricated with etching time of 0 s, 30 s, 60 s, and 90 s.

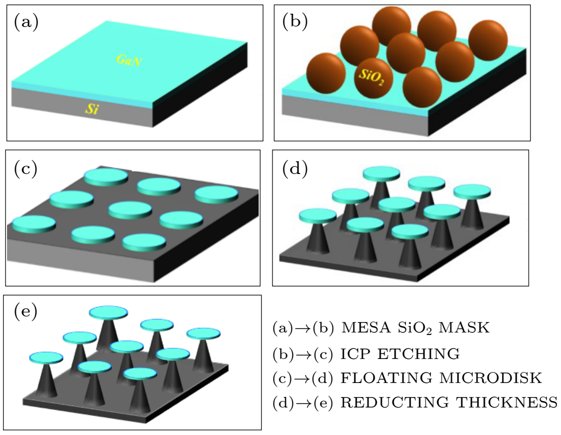

Fig. 1. Schematic fabrication process of the floating GaN microdisk: (a) Si based GaN epitaxial wafer, (b) spin-coated SiO2 microspheres, (c) etching the GaN layer to the silicon layer by ICP and removing SiO2 microspheres, (d) wet isotropic etching of silicon using the HNF etchant solution, (e) reducing the thickness of GaN with ICP etching.

A confocal micro-photoluminescence (μ-PL) spectroscopy system with a laser source and spectrometer (Princeton Instruments Acton SP2500i) was used to study the lasing emission characteristics of the floating GaN microdisks at room temperature. A neodymium-doped yttrium aluminum garnet (Nd:YAG) pulsed laser (355 nm, 10 Hz, 6 ns) was used as the excitation light source. The focused spot size of the laser beam is approximately 30 µm. A 325 nm laser (1000 Hz, 150 fs) was used to conduct time-resolved PL (TRPL) spectroscopy measurements with an Optronis GmbHSC-10 camera system.

Results and Discussion. Figure 2 shows the SEM (Hitachi SEM SU-8010) images of the GaN structures and the corresponding lasing performance. The un-etched floating GaN microdisk shown in Fig. 2(a) has a symmetric disk structure with a diameter and thickness of approximately 5 µm and 2.2 µm, respectively. The side wall of floating GaN microdisk is relatively smooth, and as we can see, the side wall of floating GaN microdisk is not steep but smooth, and the diameter on the top is smaller slightly. Under optical pumping, a broad spectrum was observed at a low pump power of 0.3 µW for the unetched samples [Fig. 2(e)], which was attributed to the spontaneous emission of GaN. As the excitation power is increased to 0.4 µW, a clear lasing mode can be observed. The center of the strongest lasing peak was at 376.3 nm with a full width at half maximum (FWHM) of 0.5 nm. A clearer resonant mode appears for a higher pumping power. The quality factor Q can be defined as

$$Q = \lambda/\Delta\lambda, \quad (1)$$

where λ and $\Delta\lambda$ represent the central wavelength and the FWHM of the lasing peak, respectively. Therefore, the lasing Q of the strongest peak was approximately 750 at an excitation power of 1.1 µW. After 30 s of ICP etching of the GaN, the thickness of the floating GaN microdisk was reduced [Fig. 2(b)]. The diameter of the floating microdisk was 5 µm, its thickness was approximately 1.9 µm, the side wall steepness was improved, and the surface remained comparable smooth. As for the corresponding lasing performance, after etching for 30 s, the center of the strongest lasing peak was at 378.4 nm and the FWHM was at 0.33 nm [Fig. 2(f)]. The lasing Q of the strongest peak was approximately 1150 at an excitation power of 1.3 µW. It increased after 30 s of etching, and the spectrum appeared with red shift. This is because of the reduction in cavity thickness, and the light confinement effect is increased in this situation. After 60 s of ICP etching of GaN, the thickness of the floating GaN microdisk was reduced further to approximately 1.7 µm [Fig. 2(c)], and the side wall steepness was further increased. However, the surface of the sidewall became poor and the diameter decreased slightly. The poor sidewall condition will decrease the lasing performance. The corresponding lasing behavior is shown in Fig. 2(g), where the center of the strongest lasing peak was at 378.64 nm and the FWHM was at 0.3 nm after etching for 60 s. The lasing Q of the strongest peak was approximately 1300 under an excitation power of 1.0 µW. The quality factor Q increased further after 60 s of etching, while the lasing mode became unclear; here, the sidewalls became rough owing to the etching. The roughness of the surface sidewall increased significantly with further increase in the etching time of GaN. After 90 s of ICP etching of GaN, the thickness of the floating GaN microdisk was reduced to approximately 1.45 µm [Fig. 2(d)], the surface and sidewall were rougher, and the diameter was reduced to less than 5 µm, which is advantageous because this device shows the best side wall steepness and the lasing performance becomes stable. After etching for 90 s [Fig. 2(h)], the center of the strongest lasing peak was shifted to 371.56 nm and the FWHM was at 0.31 nm. The lasing Q of the strongest peak was approximately 1200 under an excitation power of 1.5 µW. Blue shift of the central wavelength here was normal since the GaN materials were grown on Si with AlN as buffer layer. With the decrease of thickness of the GaN layer, the gain materials may change to AlN (with higher bandgap), then gain spectra will be blue shifted. The general conclusion in Fig. 2 is that the thinner the cavity, the greater the steepness of the structures. The Q factor increases with the decreasing cavity thickness, whereas the lasing mode stability depends on the diameter, thinness, and steepness of the cavity.

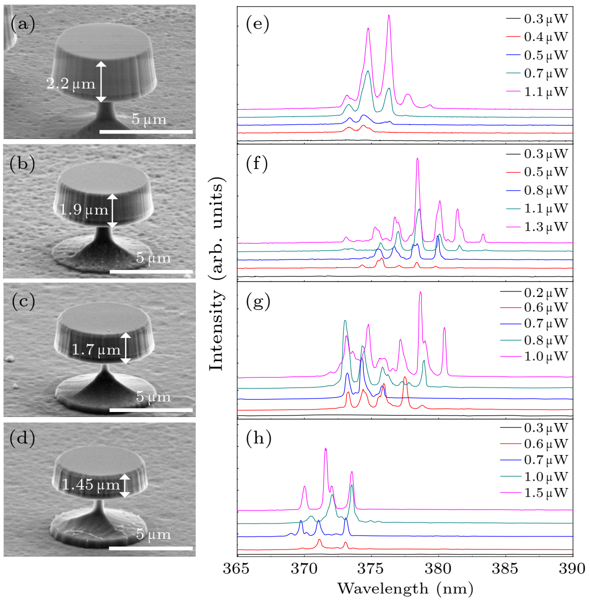

Fig. 2. Cavity thickness dependent side view SEM images of floating GaN microdisk and corresponding power dependent lasing performances: [(a), (e)] the primary samples with thickness of 2.2 μm, [(b), (f)] GaN microdisk with thickness of 1.9 μm, [(c), (g)] GaN microdisk with thickness of 1.7 μm, [(d), (h)] GaN microdisk with thickness of 1.45 μm.

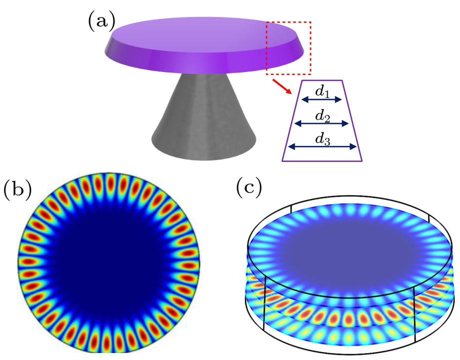

Fig. 3. (a) A simplified diagram of the GaN structure, (b) top-view simulation of GaN microdisk, (c) 3D simulation of GaN microdisk.

The quality factor of WGM lasing is determined by several factors[31] $Q^{-1} = Q_{\rm rad}^{-1} + Q_{\rm ss}^{-1} + Q_{\rm cont}^{-1} + Q_{\rm mat}^{-1}$, with $Q_{\rm rad}^{-1}$ being the intrinsic radiative (curvature) loss, $Q_{\rm ss}^{-1}$ the scattering loss on residual surface inhomogeneities, $Q_{\rm cont}^{-1}$ the loss introduced by surface contaminants, $Q_{\rm mat}^{-1}$ the material loss. Because the sidewall of the microdisk was not steep [shown in Fig. 3(a)], the Q value was expected to be strongly affected by the scattering loss of the microdisk sidewall. The scattering loss can be calculated by[31]

$$Q_{\rm ss}^{-1} = \frac{2\pi^2\sigma^2 B}{\lambda^2 D}, \tag{2}$$

where σ and B are the RMS size and correlation length of the surface of the homogeneities, respectively, D is the thickness of the cavity, and λ represents the central wavelength. The central wavelengths of the microdisk are 376.3 nm, 378.4 nm, 378.64 nm, and 371.56 nm, respectively. According to the SEM images of the floating GaN microdisk, the values of unevenness of the cavity surface were 170 nm, 180 nm, 190 nm, and 200 nm. The calculated values of $Q_{\rm ss}^{-1}$ are 4.73×10^{-4}, 5.2×10^{-4}, 5.23×10^{-4}, and 5.71×10^{-4}. The scattering loss increased with increasing etching time, which can be used to explain the changes in the Q factor.

Figure 3(a) shows the simplified diagram of the GaN structure, the top and down diameters are not same. Simulated top view of the GaN microdisk [Fig. 3(b)], with a diameter of 5 μm, the light is well confined in the cavity and surrounds the side wall of microdisk. Figure 3(c) shows a three-dimensional top view of a GaN microdisk with a diameter of 5 μm and a thickness of 1.45 μm. It can be seen that there are three modes inside the microdisk, and the light intensity of the middle mode is the strongest. The reason for this phenomenon is that due to ICP etching, the side wall of the microdisk is tilted, and multiple resonance modes will be generated [Fig. 3(a)]. The resonance mode in the middle is the strongest.

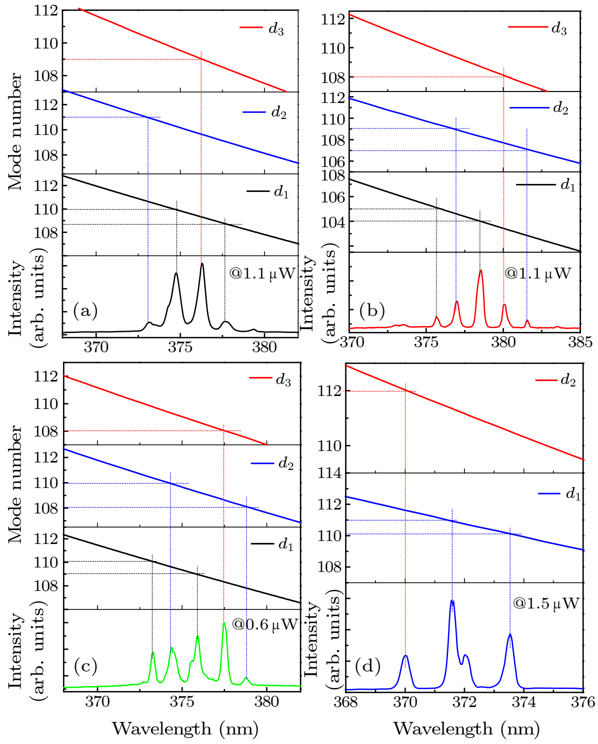

Fig. 4. The lasing spectra and calculated lasing mode number of GaN microdisk with thicknesses of (a) 2.2 μm, (b) 1.7 μm, (c) 2.2 μm, and (d) 1.45 μm.

To demonstrate the influence of diameter unevenness on mode evolution, diameter-related mode analysis was performed. The refractive index of GaN for TE-polarized light can be described by the Sellmeier dispersion equation:[32]

$$n^2 = 3.60 + \frac{1.75\lambda^2}{\lambda^2 - 0.256^2} + \frac{4.1\lambda^2}{\lambda^2 - 17.86^2}. \tag{3}$$

The lasing module equation of WGM lasing in the GaN circular microdisk is expressed as[33,34]

$$N = \pi dn/\lambda, \tag{4}$$

where n is the refractive index of GaN at a wavelength λ, d is the circular diameter of the GaN microdisk. Because the circulation path of light in the microdisk is slightly different, the diameter d corresponding to different lasing modes varies. Figure 4 shows the mode number N versus λ curves of the WGM lasing spectra before and after etching. The vertical dotted lines representing the intersection of the lasing spectra and the N–λ curves show integer numbers that correspond exactly to the lasing mode number of the WGM lasing peak. As can be seen in Fig. 4(a), for the un-etched sample under pumping power of 1.1 µW, resonant mode numbers of 108–111 for diameters of d_1 to d_3 can be obtained. When taking the sample after etching for 30 s, the resonant mode number changes to 104–109. The details of the lasing modes and diameters of each cavity are summarized in Table 1. The lasing mode number was in the range from 108 to 112.

Table 1. Summary of calculated lasing mode number and correlative diameters.

Unetched floating GaN microdisks pump power 1.1 µW		Etching time 30 s pump power 1.1 µW		Etching time 60 s pump power 0.6 µW		Etching time 90 s pump power 1.5 µW	
Diameter (µm)	Modes	Diameter (µm)	Modes	Diameter (µm)	Modes	Diameter (µm)	Modes
$d_1 = 4.9999$	110, 108	$d_1 = 4.797$	105, 104	$d_1 = 4.978$	110, 109	$d_1 = 4.984$	111, 110
$d_2 = 5.015$	111, 109	$d_2 = 4.995$	109, 107	$d_2 = 4.992$	110, 108	$d_2 = 5.003$	112
$d_3 = 4.987$	109	$d_3 = 5.014$	108	$d_3 = 4.9642$	108		

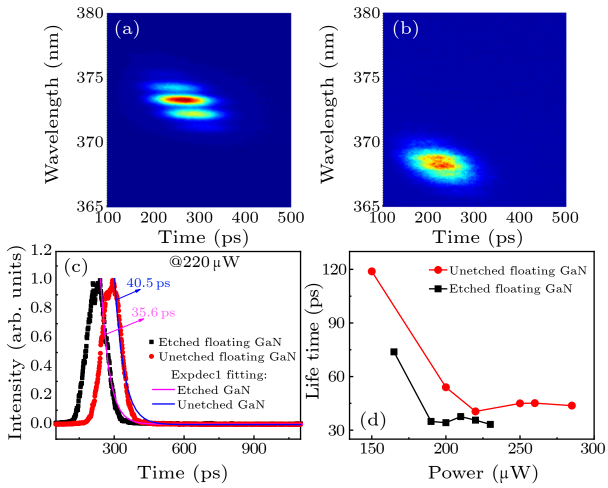

Fig. 5. (a) Stripe camera picture for the device thickness of 2.2 µm (before etching). (b) Stripe camera picture for the device thickness 1.45 µm (etching for 90 s). (c) Normalized TRPL spectra and single exponential fitting of the sample for pump power 220 µW. (d) Lifetime summary of the floating GaN microdisk with different thicknesses at different pump powers.

ICP etching can change cavity size, steepness, and surface conditions. All these parameters can influence the light emission performance of microdisk. To further demonstrate the influence of ICP etching on the lasing performance, pumping power-dependent excitation of the combination properties of samples before and after ICP etching was performed. Figures 5(a) and 5(b) show the exciton combination properties obtained by the streak camera for the samples before and after etching for 90 s under the same pumping power (325 nm fs laser at 220 µW). The resonant mode is observed in the stripe camera image in Figs. 5(a) and 5(b). The normalized TRPL spectra of the peak wavelength are presented in Fig. 5(c). Under single exponential fitting, the excitation combination lifetime is 40.5 ps for the primary sample, and 35.6 ps for the sample after etching for 90 s. As shown in Fig. 5(d), the lifetime was shortened after etching, and this conclusion did not change for other pumping powers. The increase of quality factor Q is the reason for this, and the underlying mechanism is the improvement of light confinement effect for thinner cavities. In fact, ICP etching reduces the thickness of microdisk. For example, the thickness of the primary sample was approximately 2.2 µm while it will be decreased to 1.45 µm after 90 s of etching, as shown in Fig. 2.

In summary, we have prepared a floating GaN microdisk with diameter of 5 µm and thickness of 2.2 µm by dry etching GaN and HNF solution isotropic wet etching silicon, and obtained WGM lasing in the ultraviolet range of the GaN microdisks. The thickness of GaN microdisk can be further etched using dry etching. The thickness of microdisk is reduced to 1.9 µm, 1.7 µm, and 1.45 µm after ICP etching. Lasing performance, including the quality factor Q, lifetime, and lasing mode number, is influenced by the thickness of microdisk. The resonant mode series were similar, and the Q factor first increases and then decreases, however, the lifetime decreases with decreasing the thickness of the microdisk. Overall consideration, the GaN microdisk with thickness of 1.7 µm has the highest lasing performance. Our research may benefit future development of high-quality optical active microcavities.

Acknowledgments. This work was supported by State Key Laboratory of Luminescence and Applications (Grant No. SKLA-2021-04), the Foundation of Jiangsu Provincial Double-Innovation Doctor Program (Grant No. 30644), the Natural Science Foundation of Jiangsu Province (Grant No. BK20215093), the Research Start-up Fund (Grant Nos. NY219147 and NY220181), the Postgraduate Research & Practice Innovation Program of Jiangsu Province (Grant Nos. SJCX21_0267 and SJCX22_0279).

References

[1] Rodríguez-Fernández C, Almokhtar M, Ibarra-Hernández W, de Lima J M M, Romero A H, Asahi H, and Cantarero A S 2018 *Nano Lett.* **18** 5091

[2] Almokhtar M, Emura S, Zhou Y K, Hasegawa S, and Asahi H 2011 *J. Phys.: Condens. Matter* **23** 325802

[3] Li X, Zhu G, Gao X, Bai D, Huang X, Cao X, Zhu H, Hane K, and Wang Y 2015 *IEEE Photon. J.* **7** 1

[4] Vahala K J 2003 *Nature* **424** 839

[5] Kippenberg T J, Spillane S M, Min B, and Vahala K J 2004 *IEEE J. Sel. Top. Quantum Electron.* **10** 1219

[6] Zhi Y Y, Yu X C, Gong Q, Yang L, and Xiao Y F 2017 *Adv. Mater.* **29** 1604920

[7] Cao H, Zhao Y G, Ho S T, Seelig E W, and Wang Q H 1999 *Phys. Rev. Lett.* **82** 2278

[8] Redding B, Choma M A, and Cao H 2012 *Nat. Photon.* **6** 355

[9] Wiersma D S and Cavalieri S 2001 *Nature* **414** 708

[10] Wiersma D 2000 *Nature* **406** 133

[11] Biasco S, Beere H E, Ritchie D A, Li L, Davies A G, Linfield E H, and Vitiello M S 2019 *Light Sci. Appl.* **8** 43

[12] Woodward S L, Iannone P P, Reichmann K C, and Frigo N J 1998 *IEEE Photon. Technol. Lett.* **10** 1337

[13] Marcenac D D and Carroll J E 1993 *IEEE Proc. J. Optoelectron.* **140** 157

[14] Javaloyes J and Balle S 2010 *IEEE J. Quantum Electron.* **5** 461023

[15] Savchenkov A A, Chiow S W, Ghasemkhani M, Williams S, Yu N, Stirbl R C, and Matsko A B 2019 *Opt. Lett.* **44** 4175

[16] Sandoghdar V, Treussart F, Hare J, Lefevre S V, Raimond J M, and Haroche S 1996 *Phys. Rev. A* **54** R1777

[17] Liang W, Ilchenko V S, Savchenkov A A, Matsko A B, Seidel D, and Maleki L 2010 *Opt. Lett.* **35** 2822

[18] Wang Q J, Yan C, Yu N, Unterhinninghofen J, Wiersig J, Pflügl C, Diehl L, Edamura T, Yamanishi M, Kan H, and Capasso F 2010 *Proc. Natl. Acad. Sci. USA* **107** 22407

[19] Kawabe Y, Spiegelberg C, Schülzgen A, Nabor M F, Kippelen B, Mash E A, Allemand P M, Kuwata G M, Takeda K, and Peyghambarian N 1998 *Appl. Phys. Lett.* **72** 141

[20] Shopova S I, Farca G, Rosenberger A T, Wickramanayake W M S, and Kotov N A 2004 *Appl. Phys. Lett.* **85** 6101

[21] Wu Y and Leung P T 1999 *Phys. Rev. A* **60** 630

[22] Sprenger B, Schwefel H G L, and Wang L J 2009 *Opt. Lett.* **34** 3370

[23] Chiasera A, Dumeige Y, Feron P, Ferrari M, Jestin Y, Nunzi C G, Pelli S, Soria S, and Righini G C 2010 *Laser Photon. Rev.* **4** 457

[24] Dai J, Xu C X, Ding R, Zheng K, Shi Z L, Lv C G, and Cui Y P 2009 *Appl. Phys. Lett.* **95** 191117

[25] Zhu G P, Xu C X, Zhu J, Lv C G, and Cui Y P 2009 *Appl. Phys. Lett.* **94** 051106

[26] Peng Y Y, Lu J, Peng D, Ma W, Li F, Chen Q, Wang X, Sun J, Liu H, and Pan C 2019 *Adv. Funct. Mater.* **29** 1905051

[27] Ceppe J B, Féron P, Mortier M, and Dumeige Y 2019 *Phys. Rev. Appl.* **11** 064028

[28] Nesnidal M P, Mawst L J, Bhattacharya A, Botez D, DiMarco L, Connolly J C, and Abeles J H 1996 *IEEE Photon. Technol. Lett.* **8** 182

[29] Chen L and Towe E 2006 *Appl. Phys. Lett.* **89** 053125

[30] Wu X, Li H, Liu L, and Xu L 2008 *Appl. Phys. Lett.* **93** 081105

[31] Gorodetsky M L, Savchenkov A A, and Ilchenko V S 1996 *Opt. Lett.* **21** 453

[32] Barker J A S and Ilegems M 1973 *Phys. Rev. B* **7** 743

[33] Wang S J, Huang Y Z, Yang Y D, Lin J D, Che K J, Xiao J L, and Du Y 2010 *J. Opt. Soc. Am. B.* **27** 719

[34] Yang Y D and Huang Y Z 2007 *IEEE J. Quantum Electron.* **43** 497